Turkish Journal of Physics

http://journals.tubitak.gov.tr/physics/

Research Article

Turk J Phys
(2020) 44: 247 – 255

doi:10.3906/fiz-1911-14

Local vibrational modes of natural isotopes of substitutional oxygen in CdTe

Enver TARHAN[1,*], **Anant K. RAMDAS**[2]
[1]Department of Physics, Faculty of Science, İzmir Institute of Technology, İzmir, Turkey
[2]Department of Physics, Purdue University, West Lafayette, IN, USA

Received: 26.11.2019 • **Accepted/Published Online:** 05.04.2020 • **Final Version:** 22.06.2020

Abstract: We investigated the localized vibrational modes (LVM) of natural oxygen containing ^{16}O, ^{17}O, and ^{18}O isotopes at a substitutional tellurium site in cadmium telluride using infrared absorption spectroscopy at cryogenic temperatures. The main absorption peak observed at 350 cm^{-1} was formerly attributed to a fundamental LVM mode (ν_0) of oxygen at a tellurium site. The relatively weak absorption peaks observed at 331 cm^{-1} and 340 cm^{-1} are assigned as the same ν_0 mode of the ^{17}O and ^{18}O isotopes, respectively, based on their relative intensities and spectral positions. The spectral positions were confirmed with theoretical calculations using a linear chain model where the peak position at 350 cm^{-1} was taken as the reference for the ^{16}O isotope. From a least square analysis of the observed peak positions we were able to calculate the force constants from perturbation theory. A Lorentzian line shape analysis of each ν_0 absorption peak, considering the effects of isotopic mass and natural abundance variations of the host Cd atoms, was also carried out to further confirm their assignments. Reasonably good line shape fittings were obtained for ν_0 modes of all isotopes of oxygen.

Key words: Local vibrational modes, oxygen impurities, cadmium telluride

1. Introduction

In the study of defects in semiconductors, local vibrational modes (LVMs) of impurity atoms provide valuable information about the host material as well as impurity atoms in it. LVMs arise when an impurity atom at a substitutional site is much lighter than any of the host atoms in elemental and compound semiconductors provided that the force constant strengths between the impurity and the host atoms are not much different from those among the host atoms themselves [1]. For example, Li impurities in CdTe replacing either Cd or Te atoms of the host produce well defined localized vibrational modes [2]. Many local modes of light impurities are reported in the literature, such as those of Be in ZnTe, ZnSe, ZnS, and CdTe [3–4] and those of S, Be, and Mg in $Zn_xCd_{1-x}Te$ [5]. Infrared absorption studies of these modes provide clear insight into the nature of such defects and their surroundings [1,6–7].

CdTe is a very important technological material especially for their infrared detector applications [8] and solar cells [9]. A knowledge of the host structure as well as defects in it is of great importance to understand and improve its optoelectronic properties for such device applications. Oxygen is a well-known impurity giving rise to several defect structures in CdTe. A detailed analysis of the LVM spectra of oxygen defect centers in CdTe is given by Chen et al. using high resolution Fourier transform infrared absorption spectroscopy [10]. CdTe is a

*Correspondence: envertarhan@iyte.edu.tr

tetrahedrally coordinated semiconductor. In its zinc blende lattice, an oxygen impurity atom replacing a host Te atom, named the "O_{Te} center", shows a sharp peak centered at about 350 cm^{-1}, called the "ν_0 peak", in the infrared absorption spectrum as reported by Chen et al. In the present study, we report the effect of natural isotopes of oxygen, namely ^{16}O, ^{17}O, and ^{18}O, on the ν_0 peak which eventually provides further insight into the properties of the host material.

2. Theoretical discussions and experimental methods

2.1. Energy states of a substitutional light impurity in a zinc blend crystal

Analytical calculations of localized vibrational mode frequencies were carried out by several researches for a light impurity atom replacing a host atom with a heavier mass [1,11,12]. In the case of a zinc blende structure, such as that of CdTe, ZnTe, or ZnS, the potential energy function for a light impurity atom at a T_d site can be approximated by that of an unharmonic oscillator as given by Elliot et al. [13]:

$$V(T_d) = \frac{k}{2}\left(x^2+y^2+z^2\right) + B(xyz) + D_1\left(x^4+y^4+z^4\right) +$$

$$D_2\left(x^2y^2+x^2z^2+y^2z^2\right) + \ldots, \tag{1}$$

where (x, y, z) are cubic coordinates and k, B, D_1, and D_2 are parameters (may also be called the "force constants") which are to be obtained from theoretical fits to experimental data. The energies are calculated using the perturbation theory, treating the cubic term to the second order and the quartic terms (4th power terms) to the first order with an assumption that the motion of the impurity atom does not affect that of the host atoms beyond its nearest neighbors (NN) or next nearest neighbors (NNN). Considering only the nearest neighbors, energies of an impurity oscillator at a Td site are found as;

$$E_N = \hbar\sqrt{\frac{k}{M'}}(N+3/2) - \frac{\hbar^2}{24k^2M'}\lambda B^2 + \frac{\hbar^2}{2kM'}(\mu_1 D_1 + \mu_2 D_2), \tag{2}$$

where $N = 0, 1, 2, \ldots$ and $M' = MM_L/(M+M_L)$ is the reduced impurity mass. M is the mass of the oscillating impurity and M_L is the *lattice interaction mass*, representing the effective mass of the neighboring lattice atoms. In the analyses of an absorption spectrum of such an impurity, M_L is usually treated as a fitting parameter to experimental data which is between one and four times the mass of a neighboring lattice atom. The parameters λ, μ_1, and μ_2 were calculated from the perturbation theory and given in Table 8 of Elliot et al.

When various isotopes of an impurity element exist, such as oxygen in CdTe with three different natural isotopes, namely ^{16}O, ^{17}O, and ^{18}O, with natural abundances of 99.8%, 0.04%, and 0.2%, respectively, one expects shifts from higher to lower frequencies with increasing isotopic mass for the same type of local mode vibration. At the same time, the observed infrared absorption peak intensity of an isotope would be scaled with the natural abundance of that isotope. The only difference being the isotopic mass of the impurity, one can easily deduce the frequency position of the LVM of a particular isotope from a well-known one in the infrared (IR) spectrum. In the crude approximation of a harmonic oscillator in the diatomic linear chain model, the frequency for a particular isotope with mass M is given as

$$\omega = \sqrt{\frac{k}{\mu}}, \qquad \mu = \frac{1}{M_L} + \frac{1}{M}, \tag{3}$$

where the effective lattice mass M_L is as given above. Thus, for the same effective lattice mass M_L and for the same force constant k, the LVM frequency ω_j for a particular oxygen isotope with mass M_j can be expressed in terms of a known LVM frequency ω_i of an isotope with mass M_i as [11]

$$\omega_j = \sqrt{\frac{M_i}{M_j}}\,\omega_i \tag{4}$$

The host atoms, on the other hand, may have their own isotopic configurations. For a particular O_{Te} center, there are four nearest neighbor (NN) Cd atoms at a given Te site, each of which are positioned at the corners of a tetragon whose center is at the impurity site. All corners of a tetragon are equivalent to one another, as seen by a point in its center (Te site in CdTe). In group theory, such a point has a T_d site symmetry. However, isotopic variations in the masses of neighboring Cd atoms will cause slight variations in the lattice interaction mass M_L which leads to variations in the in the LVM frequencies. Since there are 8 different stable isotopes of Cd with varying natural abundances, the total number of possible isotopic configurations for all possible mass variations of Cd becomes $N = 8^4 = 4096$, albeit many of them being degenerate. Then, for any given vibrational frequency for a particular isotopic combination of NN Cd atoms, all possible LVM frequencies for all possible NN Cd configurations can be computed by taking into account all possible mass combinations in the NN Cd sites along with proper weight factors to determine the relative intensities, which are to be calculated from the natural abundances for a particular NN Cd configuration. Finally, the calculated line shape of an LVM peak for a particular oxygen isotope will be the sum of all possible individual LVM peaks obtained for all NN Cd mass combinations. In this work, for each NN Cd mass configuration, the effective lattice mass M_L was calculated as the average of four NN Cd atoms multiplied by a proper weight factor A for a particular O_{Te} impurity to account for the effect of the whole lattice in Equation 3. Then, for a particular combination n (n ranges from 1 to N) of NN Cd atoms a frequency ω_n was obtained from Equation (3). Next, a Lorentzian function centered at that frequency was obtained as

$$y_n(\omega) = \frac{h_n}{1 + \left(\frac{\omega - \omega_n}{\Gamma}\right)^2}, \tag{5}$$

where h_n represents the probability of the nth NN Cd configuration (which is to be found by multiplying their natural abundances) and Γ is the full width of the Lorentzian peak at half maximum (FWHM). Finally, the line shape of an LVM absorption peak of a particular oxygen isotope was calculated as the sum of all Lorentzians for all NN Cd configurations; that is

$$\alpha_{calc} = \sum_{n=1}^{N} y_n. \tag{6}$$

This line shape function was then fitted to the corresponding absorption data.

2.2. Experimental methods

Crystals of CdTe were grown by a floating zone vertical Bridgeman technique. A high purity CdTe powder and appropriate amounts of TeO_2 or CdO were placed in a sealed quartz ampoule along with a small piece of seed CdTe crystal. A 5 °C/cm temperature gradient was used in a two-zone furnace. The details of the growth

procedure is given elsewhere [10]. After the growth, a CdTe crystal ingot was cut into many sample pieces, each one being about half a centimeter in diameter with a few millimeter thickness. Then, samples were polished with carborundum and a 3 micron diamond paste on a turn table. A wedge was introduced during polishing to suppress channeling in the transmission spectrum of a sample. A very high resolution Fourier Transform Spectrometer (FTS) (ABB BOMEM DA3.002) capable of a maximum resolution of 0.0026 cm^{-1} was used to obtain the transmission spectrum [14] of a sample from which absorption coefficient was calculated using the well-known equation [15];

$$\alpha = \frac{1}{d} ln \left\{ \frac{1-R^2}{2T} + \sqrt{R^2 + \left(\frac{(1-R^2)}{2T} \right)^2} \right\}, \tag{7}$$

where d is the thickness of the sample, T, transmission, is the ratio of transmitted light intensity to that of the incident one, while R, reflection, is the ratio of the reflected intensity to the incident intensity. R can be calculated from the following equation:

$$R = \frac{(n-1)^2 + \kappa^2}{(n+1)^2 + \kappa^2}, \tag{8}$$

where n is the refractive index of the sample and κ is the extinction coeffiecient. We calculated R from the given values of n and κ in the literature. After measuring the film thickness d, we calculated the absorption coefficient of the sample from Equation (7). A composite Si bolometer was used as the detector in the 10–700 cm^{-1} range. Samples were cooled down to 5 K in a Janis 10 D Supervaritemp optical crystal which allows transmission or reflection measurements in the temperature range from 1.8 K to 300 K in the optical range of 10 cm^{-1} to 50,000 cm^{-1} [16].

3. Results and discussion

A high resolution absorption spectrum of an oxygen doped CdTe (CdTe:O) sample, with a thickness of 0.1197 cm, measured with 0.05 cm^{-1} resolution at 5 K is shown in Figure 1. The sharp and intense absorption peak centered at 349.8 cm^{-1} (labeled as ν_0, O16) is attributed to a local vibrational mode of ^{16}O impurity substitutionally replacing a Te atom in the host CdTe lattice, i.e., the O_{Te} center [6]. The inset between 328 cm^{-1} and 342 cm^{-1} is the absorption coefficient of the same sample but multiplied by 50 for clarity. The weak absorption peaks centered at 331.12 cm^{-1} and 340.05 cm^{-1}, as indicated by pointing arrows in the inset, are assigned as the fundamental ν_0 local vibrational modes of ^{18}O and ^{17}O isotopes at substitutional Te sites, respectively, based on their relative intensities, spectral positions and line shapes. Also seen in Figure 1 is a relatively weak peak centered at 695.71 cm^{-1} and labeled as $2\nu_0$ which was assigned as the second harmonic of the ν_0 local vibrational mode of ^{16}O isotope by Chen et al. [10]. The absorption coefficient in that region is multiplied by 5 for clarity.

Figure 2 gives the absorption spectrum of the ν_0 mode of ^{16}O isotope at a Te site along with the theoretically calculated Lorentzian line shape fitting curve. The fittings were carried out in the spirit of the harmonic oscillator approximation of a linear chain model, as discussed in the theoretical section. To consider the effect of the nearest neighbors on the vibrational motion of an oxygen atom at a Te site in CdTe, all possible combinations of the NN Cd isotopes were taken into account with proper weight factors which were obtained from the natural abundances of the isotopes of Cd. Table 1 gives the natural abundances of stable oxygen and

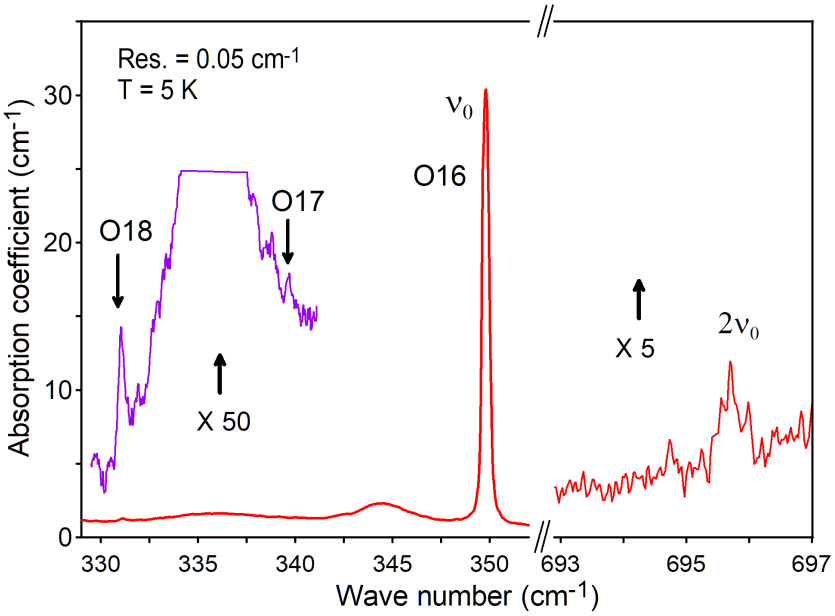

Figure 1. High resolution absorption spectrum of a CdTe:O sample displaying the local vibrational modes 0 for all three isotopes of oxygen along with the second harmonic mode 2 0 for 16O at a Te site.

cadmium isotopes used for the calculations. According to group theory, in T_d site symmetry, the ground state of an unharmonic oscillator, whose energies are given by Equation (2), has Γ_1 symmetry which means that an electric dipole transition can only terminate at excited states with Γ_5 symmetry. Hence, the only possible transitions to the first and second excited states are of the form $\Gamma_1 \rightarrow \Gamma_5$.

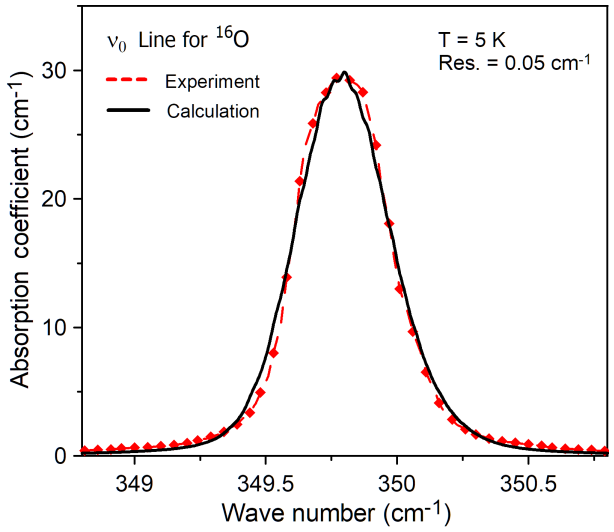

Figure 2. Absorption spectrum of fundamental ν_0 mode due to 16O local vibrations (dashed lines with square symbols) along with the calculated theoretical fit (continuous dark curve).

Table 2 gives the calculated parameters (force constants) k, B, D_1, D_2, and the lattice effective mass M_L of the theoretical energy levels, given by Equation (2). These parameters were found by treating them as

Table 1. Stable cadmium and oxygen isotopes along with their masses in terms of atomic mass unit (amu) and natural abundances (NA: 1 being 100%).

Isotope	^{106}Cd	^{108}Cd	^{110}Cd	^{111}Cd	^{112}Cd	^{113}Cd
Mass (amu)	105.906459	107.904184	109.903002	110.904178	111.902757	112.904402
NA	0.0125	0.0089	0.1247	0.128	0.2411	0.1223
Isotope	^{114}Cd	^{116}Cd	^{16}O	^{17}O	^{18}O	
Mass (amu)	113.903359	115.904756	15.9949146	16.9991317	17.9991610	
NA	0.2875	0.0751	0.99762	0.000377	0.00205	

fitting parameters in a least square analyses procedure described below. The energy parameters μ_1, μ_2, and λ used for the ground state (Γ_1) and the first and the second excited Γ_5 states were the same as those given in Table 8 of Elliot et al. The fittings were carried out by equating the energy differences, found from Equation (2) (N = 0 to N = 1 for ν_0 and N = 0 to N = 2 for $2\nu_0$) to the observed energies of ν_0 and $2\nu_0$ modes from the absorption spectrum for each isotope of oxygen. The same set of fitting parameters for all isotopes were assumed. Then, a nonlinear least square fitting algorithm was applied to obtain a set of best fitting force constants. To improve the computational accuracy, we guessed the spectral positions of the second harmonic ($2\nu_o$) absorption peaks for ^{17}O and ^{18}O isotopes from the spectral position of the $2\nu_o$ peak of ^{16}O isotope using Equation (4). Since the later was observed at 695.7 cm^{-1}, the others were calculated to be at 677.5 cm^{-1} and 660 cm^{-1} for ^{17}O and ^{18}O isotopes, respectively. Note that, in order to observe these peaks experimentally, one either needs much higher oxygen doping concentrations, which might cause a change in the crystal and electronic band structures, or one can try to enrich ^{17}O and ^{18}O isotopes in a specimen using enriched oxygen sources during the growth. For comparison, Table 2 also displays the results for Mg isotopes at Te sites which are reprinted from Ref. [7]. One should regard the fact that both Mg and O atoms have similar sizes, albeit force constants may vary slightly due to varying bond strengths resulting from their electronic configurations. Nevertheless, we can say that our results are close to those obtained for Mg isotopes in CdTe. The effective Cd mass, neighboring an oxygen atom, is found to be 208 atomic mass unit (amu) which is almost twice as much as that of a single Cd atom at a neighboring site. A similar effective Cd mass was also obtained in Ref. [7] as given in Table 2.

Table 2. Force constants for the unharmonic potential energy function for local vibrations of O_{Te} and Mg_{Te} (Ref. [7]) impurities at a T_d site symmetry obtained from a least square fitting of the observed peak positions to those predicted from Equation (2) (amu: atomic mass units).

Parameters of Equation (2)	O_{Te} This work	Mg_{Te} Ref. [7]
k $\left(10^5 dyne/cm\right)$	1.115	0.808
B $\left(10^{13} erg/cm^3\right)$	-1.538	-1.097
D_1 $\left(10^{20} erg/cm^4\right)$	-7.756	-1.593
D_2 $\left(10^{20} erg/cm^4\right)$	-8.899	9.007
M_L(amu)	208.292	168

Figure 3 gives the absorption peaks for the ν_0 mode of ^{17}O (a) and ^{18}O (b) isotopes along with the theoretical Lorentzian line shape fits calculated in the same way as that for ^{16}O. Since signal to noise ratio

was very small for these two peaks due to very small natural abundances of ^{17}O and ^{18}O isotopes, first, a linear background subtraction was carried out then, the signal to noise ratio was improved computationally by replacing a particular absorption data point at a particular wavelength with the average of several nearest neighbor absorption data values. It is seen that the frequency position of the peaks for the ^{17}O and ^{18}O isotopes are consistent with the results given by Equation (4) where the intense ^{16}O peak centered at 349.8 cm^{-1} was used as the reference peak to locate the frequency positions for the other two isotopes of oxygen. In addition, the relative intensities and line shapes are also consistent, especially so for the ^{16}O and ^{18}O isotopes since natural abundances for them are high enough to suppress the noise. However, the consistency in the line shape is not very good for the ^{17}O isotope due to its natural abundance being too small to produce a strong enough absorption peak over the noise level.

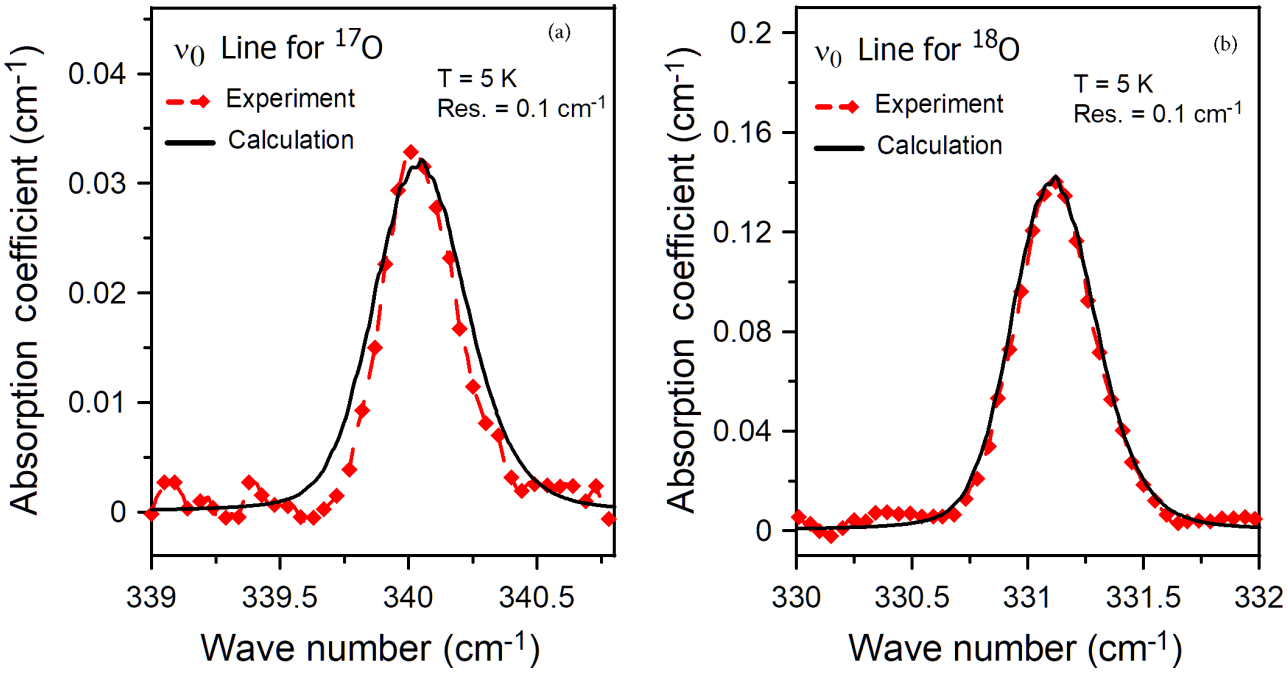

Figure 3. Absorption peaks due to local vibrational mode ν_0 ; (a) for ^{17}O and (b) for ^{18}O isotopes along with calculated fitting curves.

Table 3 displays the results of the calculated Lorentzian line shape fitting parameters for all three isotopes of oxygen. Calculated abundance, CA, is equal to the area of a ν_0 peak for an oxygen isotope divided by the sum of the areas of all ν_0 peaks for all oxygen isotopes. The values for the dominant parameter k (the harmonic force constant) found from the least square fitting procedure (Table 2) and from the line shape analyses (Table 3) are in a very good agreement ($1.15\,x\,10^5$ dyne/cm for the first method versus $1.035\,x\,10^5$ dyne/cm for the later), further confirming our results.

When we compare the natural abundances (NA) of oxygen isotopes given in Table 1 with the calculated abundances (CA) in Table 3, we see a reasonably good agreement. Although the numbers relatively seem to be quite different for ^{17}O and ^{18}O isotopes, one should remember that these are very small in concentration and the differences are only of the order of 0.01% for each isotope. Calculated relative abundances of ^{17}O and ^{18}O are also in good agreement with those for the natural ones. We notice that the effective lattice mass

Table 3. Results of the line shape fitting calculations to the observed peaks for all isotopes of oxygen (CA: calculated abundance).

Parameters for $k = 1.035 \times 10^5$ (dyne/cm)	^{16}O	^{17}O	^{18}O
$\Gamma\,(cm^{-1})$	0.043	0.04	0.04
$\omega_{max}\,(cm^{-1})$	349.8	340.05	331.12
μ (amu)	14.35	15.184	16.01
M_L(amu)	139.51	142.23	145.24
CA	0.995	0.0009	0.004

M_L values found from the line shape fitting analyses are somewhat different from those found using Equation (2) as described above. The main difference is probably due to the fact that the force constants given in Table 3 are approximately true since we ignored the contributions from the next nearest neighbors and so on. In addition, the linear chain model may not precisely predict the frequencies since it ignores three dimensional nature of the oscillations. Thus, one should consider the values of the parameters listed in Table 3 as approximations to real ones. One should regard the fact that the most important contribution to the energy of a localized vibrational mode, as given by Equation (2), comes from the first term which is the harmonic one. The unharmonic contributions are found from the perturbation theory and their contributions are relatively smaller than the harmonic one. In fact, for calculation purposes, we kept the parameter k (harmonic force constant) the same for all isotopes of oxygen in the line shape analyses for self-consistency.

4. Conclusions

The peak located around 349.8 cm^{-1} in the absorption spectrum of an oxygen doped CdTe sample has been observed in many absorption experiments involving CdTe. It was assigned to a local vibrational mode of an oxygen impurity at a Te site by Chen et al. [10]. In this work, we carried out detailed analyses of this peak using both perturbation theory as given by Elliot et al. [13] and by a Lorentzian line shape fitting for each isotopic configuration of neighboring Cd atoms for a particular isotope of oxygen. We were able to obtain an especially good agreement for the harmonic force constant k for all isotopes of oxygen. This value of k is also very close to those obtained for other impurities such as Ca and Mg at a Te site in CdTe, further confirming the results of our analyses and interpretations for the assignments of the related absorption peaks. The parameters of the perturbation theory [Equation (2)] also seem to be in good agreement with those obtained for other impurity atoms such as Mg at Te sites. We were able to make the first identification and analyses of the fundamental ν_0 local vibrational mode of ^{17}O and ^{18}O isotopes. However, further research is necessary to assert these assignments and our findings more firmly since the natural abundances of ^{17}O and ^{18}O isotopes are very small, thus, not leading to strong absorption peaks. One also needs to observe the second harmonic modes of ν_0 for ^{17}O and ^{18}O isotopes in order to obtain a better set of fitting parameters to understand the nature of these local vibrational modes.

Acknowledgement

We would like to acknowledge the National Science Foundation (Grant Nos. DMR-0102699 and ESC-0129853) for supporting the research reported this paper.

References

[1] Barker AS, Sievers AJ. Optical studies of the vibrational properties of disordered solids. Reviews of Modern Physics 1975; 47 (S2): S1-S179.doi: 10.1103/RevModPhys.47.S1.2

[2] Zielinska R, Krol A, Nazarewicz W. Lithium-related point defects in CdTe. Journal of Physics C: Solid State Physics 1984; 17 (29): 5209-5218. doi: 10.1088/0022-3719/17/29/020

[3] Manabe A, Ikuta Y, Mitsuishi A, Komiya H, Ibuki S. Infrared absorption and Raman scattering due to localized vibrational mode of Be in zinc-chalcogenides. Solid State Communications 1971; 9 (17): 1499-1502. doi: 10.1016/0038-1098(71)90165-7

[4] Hayes W, Spray ARL. Infra-red absorption of beryllium in cadmium telluride: I. Journal of Physics C: Solid State Physics 1969; 2 (2): 1129-1136. doi: 10.1088/0022-3719/2/7/305

[5] Harada H, Narita SJ. Lattice vibration spectra of ZnxCd1-xTe alloys. Journal of the Physical Society of Japan 1971; 30 (6): 1628-1639. doi: 10.1143/JPSJ.30.1628

[6] MayurAJ, Sciacca MD, Kim H,Miotkowski I, Ramdas AK et al. Local and gap modes of substitutional 3d transition-metal ions in zinc-blende and wurtzite II-VI semiconductors. Physical Review B 1996; 53 (19): 12884-12888.doi: 10.1103/PhysRevB.53.12884

[7] Sciacca MD, Mayur AJ, Shin N, Miotkowski I, Ramdas AK et al. Local vibrational modes of substitutional Mg^{2+}, Ca^{2+}, and S^{2-} in zinc-blende and wurtzite II-VI semiconductors. Physical Review B 1995; 51 (11): 6971-6978. doi: 10.1103/PhysRevB.
51.6971

[8] Rogalski A. Infrared detectors: an overview. Infrared Physics & Technology 2002; 43 (3): 187–210.doi: 10.1016/S1350-4495(02)00140-8

[9] Ferekides CS, Marinskiy D, Viswanathan V, Tetali B, Palekis V et al. High efficiency CSS CdTe solar cells. Thin Solid Films 2000; 361 (361): 520-526. doi: 10.1016/S0040-6090(99)00824-X

[10] Chen G, Miotkowski I, Rodriguez S, Ramdas AK. Control of defect structure in compound semiconductors with stoichiometry: Oxygen in CdTe. Physical Review B 2007; 75 (12): 125204-1-125204-10. doi: 10.1103/PhysRevB.75.125204

[11] Stavola M.Chapter 3 Vibrational spectroscopy of light element impurities in semiconductors.In Willardson RK and Weber ER (editors). Semiconductors and Semimetals Volume 51B. New York, NY, USA: Academic Press, 1999, pp. 153-224.

[12] McCluskey MD. Local vibrational modes of impurities in semiconductors. Journal of Applied Physics 2000; 87 (1): 3593-3612.doi: 10.1063/1.372453

[13] Elliott RJ, Hayes W, Jones GD, MacDonald HF, Sennett CT. Localized vibrations of H– and D– ions in the alkaline earth fluorides. Proceedings of the Royal Society A 1965; 289 (1412): 1-33. doi: 10.1098/rspa.1965.0246

[14] ABB BOMEM Inc., 585 Charest BLVD East, Suite 300, Québec, Canada, G1K 9H4.

[15] Barnes RB, Czerny M. Concerning the reflection power of metals in thin layers for the infrared. Physical Review 1931; 38 (2): 338-345. doi: 10.1103/PhysRev.38.338

[16] Janis Research Company, Inc., 2 Jewel Drive, Wilmington, MA 01887-0896. USA